Many-polaron effects in the Holstein model

Sanjoy Datta, Arnab Das, and Sudhakar Yarlagadda
Saha Institute of Nuclear Physics, Calcutta, India
(Received 28 March 2005; published 30 June 2005)

We derive an effective polaronic interaction Hamiltonian, exact to second order in perturbation, for the spinless one-dimensional Holstein model. The small parameter is given by the ratio of the hopping term (t) to the polaronic energy ($g^2\omega_0$) in the whole region of validity for our perturbation; however, the exception is the regime of extreme antiadiabaticity ($t/\omega_0 \leqslant 0.1$) and small electron-phonon coupling ($g<1$) where the small parameter is t/ω_0. We map our polaronic Hamiltonian onto a next-to-nearest-neighbor interaction anisotropic Heisenberg spin model. By studying the mass gap and the power-law exponent of the spin-spin correlation function for our Heisenberg spin model, we analyze the Luttinger liquid to charge-density wave transition at half filling in the effective polaronic Hamiltonian. We calculate the structure factor at all fillings and find that the spin-spin correlation length decreases as one deviates from half filling. We also extend our derivation of polaronic Hamiltonian to d dimensions.

DOI: 10.1103/PhysRevB.71.235118 PACS number(s): 71.38.−k, 71.45.Lr, 71.30.+h, 75.10.−b

I. INTRODUCTION

Understanding the many-body aspects of the Holstein model[1] has been a long-standing open problem. Significant progress has been made in understanding the single-polaron problem through analytic treatments in the small- and large-polaron limits and numerical approaches in the intermediate-size case.[2] While studies of the many-polaron problem, involving spin degrees of freedom, yielded interesting insights for bipolarons and their phase transitions,[2,3] the simpler case of the spinless many-polaron problem has received only scant attention.[4] With the renewed interest in strongly correlated manganite systems[5] (which are of high electronic density when the electron-phonon interactions are supposed to be important) it is imperative that the effective interaction between polarons be understood so that a serious attempt at explaining the rich phase diagram of these systems can be made. Although studying manganites demands knowledge of the effective Jahn-Teller polaronic interaction, in the low-doped case the effective Hamiltonian at 0 K for the occupied states can be taken as a Holstein model.[6] Thus a good understanding, involving exact results, of the simpler effective polaronic interaction for the Holstein model, which has been elusive so far, is highly desirable. Furthermore, an effective polaronic Hamiltonian even in the simplest spinless one-dimensional (1D) case would also be quite useful for modeling Luttinger liquid (LL) to charge-density wave (CDW) transitions in half-filled systems. Quasi-1D organic conjugated polymers [such as $(CH)_x$], charge transfer salts [such as tetrathiafulvalene-tetracyanoquinodimethane (TTF-TCNQ)], and inorganic blue bronzes[7] (e.g., $K_{0.3}MoO_3$) are good candidates for such broken symmetry in the ground state, leading to unit cell doubling.

The present paper, using the Lang-Firsov transformation,[8] provides a transparent perturbative approach to deriving the effective Hamiltonian of interacting polarons in d dimensions when the band narrowing is significant. The resulting polaronic Hamiltonian, exact to second order in perturbation, is studied in 1D at 0 K for density-density correlation effects. The correlation function exponent of the concomitant quasi-long-range order is demonstrated to be useful in characterizing the Luttinger liquid and the charge-density-wave phases of the system.

II. EFFECTIVE POLARONIC HAMILTONIAN

We begin in 1D by taking the unperturbed Hamiltonian to be the noninteracting polaronic term[9]

$$H_0 = \omega_0 \sum_j a_j^\dagger a_j - \omega_0 g^2 \sum_j c_j^\dagger c_j - J_1 \sum_j (c_j^\dagger c_{j+1} + \text{H.c.}), \quad (1)$$

with the perturbation being

$$H' = \sum_j H_j = -J_1 \sum_j (c_j^\dagger c_{j+1} \{\mathcal{S}_+^{j\dagger} \mathcal{S}_-^j - 1\} + \text{H.c.}), \quad (2)$$

where H_0+H' make up the Lang-Firsov transformed Holstein Hamiltonian and c_j (a_j) is the fermionic (phononic) destruction operator, ω_0 the Debye frequency, $\mathcal{S}_\pm^j = \exp[\pm g(a_j - a_{j+1})]$, $J_1 = t\exp(-g^2)$, with t being the hopping term, and $g^2\omega_0$ the polaronic binding energy. The eigenstates are given by $|n,m\rangle \equiv |n\rangle_{el} \otimes |m\rangle_{ph}$ with $|0,0\rangle$ being the ground state with zero phonons. The eigenenergies are $E_{n,m} = E_n^{el} + E_m^{ph}$. Since $\langle 0,n'|H'|n,0\rangle = 0$, the first-order perturbation term is zero and the relevant excited states correspond to states with nonzero phonons. Next, we represent $|m\rangle_{ph}$ in real space as phononic excitations at different sites with one phonon state being $a_j^\dagger|0\rangle_{ph}$, which is N-fold degenerate and can correspond to any site j. On the other hand, the electronic state $|n\rangle_{el}$ is represented in the momentum space. We will now calculate second-order perturbation terms *exactly*:

$$E^{(2)} = \sum_{l,j} \sum_{n,m} \frac{\langle 0,0|H_l|n,m\rangle\langle m,n|H_j|0,0\rangle}{E_{0,0} - E_{n,m}}.$$

Now $E_n^{el} - E_0^{el} \sim J_1$ and $\Delta E_m \equiv E_m^{ph} - E_0^{ph}$ is a nonzero integral multiple of ω_0. Assuming $J_1 \ll \omega_0$ (which certainly is true for realistic values of $2 < t/\omega_0 < 4$ and $6 < g^2 < 10$ found in man-

ganites) and using $\Sigma_n|n\rangle\langle n|=I$ we get the corresponding second-order term in the effective Hamiltonian for polarons to be

$$H^{(2)}=\sum_{l,j}\sum_{m}\frac{\langle 0|_{ph}H_l|m\rangle_{ph}\langle m|_{ph}H_j|0\rangle_{ph}}{-\Delta E_m}.$$

In the above equation, the term H_j produces phonons at sites j and $j+1$. Hence, to match that, its counterpart H_l should produce phonons in at least one of the two sites j and $j+1$. Thus the index $l=j-1$, j, or $j+1$. Next on defining $P_{\pm}(j;m)\equiv\langle 0|_{ph}\mathcal{S}_{\pm}^{j}-1|m\rangle_{ph}$ and $b_j\equiv c_j^{\dagger}c_{j+1}$ we get

$$\begin{aligned}H^{(2)}=&-\sum_{j,m}\frac{J_1^2}{\Delta E_m}[\{b_j^{\dagger}b_jP_+(j;m)+b_{j-1}b_jP_-(j-1;m)\\&+b_{j+1}b_jP_-(j+1;m)\}P_+^{\dagger}(j;m)+\{b_jb_j^{\dagger}P_-(j;m)\\&+b_{j-1}^{\dagger}b_j^{\dagger}P_+(j-1;m)+b_{j+1}^{\dagger}b_j^{\dagger}P_+(j+1;m)\}P_-^{\dagger}(j;m)].\end{aligned}\tag{3}$$

Then using $(a^{\dagger})^n|0\rangle=\sqrt{n!}|n'\rangle$ with $|n'\rangle$ being a state with n phonons we get the effective polaronic Hamiltonian to be

$$\begin{aligned}H_{eff}^{pol}=&-g^2\omega_0\sum_j n_j-J_1\sum_j(c_j^{\dagger}c_{j+1}+\text{H.c.})\\&+J^z\sum_j n_jn_{j+1}+2J_2\sum_j(c_{j-1}^{\dagger}n_jc_{j+1}+\text{H.c.})\\&-J_2\sum_j(c_{j-1}^{\dagger}c_{j+1}+\text{H.c.})-J^z\sum_j n_j,\end{aligned}\tag{4}$$

where $J^z\equiv(J_1^2/\omega_0)[4f_1(g)+2f_2(g)]$ and $J_2\equiv(J_1^2/\omega_0)f_1(g)$ with $f_1(g)\equiv\Sigma_{n=1}^{\infty}g^{2n}/(n!n)$ and $f_2(g)\equiv\Sigma_{n=1}^{\infty}\Sigma_{m=1}^{\infty}g^{2(n+m)}/[n!m!(n+m)]$. It is of interest to note that the *single* polaronic energy part of the above Hamiltonian matches with the self-energy expression at $k=0$ obtained by Marsiglio[10] and the self-energy at a general k by Stephan[11] and lends credibility to our results. Furthermore, in the work of Hirsch and Fradkin,[12] the coefficient of nearest-neighbor interaction agrees with our coefficient J^z for large values of g while the coefficients of the next-to-nearest-neighbor (NNN) hopping are in disagreement with ours and the results of Refs. 10 and 11. Next we make the connection that, on using the Wigner-Jordan transformation $\sigma_i^+=\Pi_{j<i}(1-2n_j)c_i^{\dagger}$, we can map the effective polaronic Hamiltonian exactly (up to a constant) onto the following NNN anisotropic Heisenberg spin chain:

$$\begin{aligned}H_{eff}^{spin}=&-g^2\omega_0\sum_j\sigma_j^z-J_1\sum_j(\sigma_j^+\sigma_{j+1}^-+\text{H.c.})\\&+J^z\sum_j\sigma_j^z\sigma_{j+1}^z-J_2\sum_j(\sigma_{j-1}^+\sigma_{j+1}^-+\text{H.c.}),\end{aligned}\tag{5}$$

where the coefficient of the first term represents coupling to a longitudinal magnetic field. Although the NNN interactions in the above Hamiltonian do not produce frustration, nevertheless the Hamiltonian cannot be solved by the coordinate Bethe ansatz.[13] Hence we have recourse to analyzing the properties of the effective Hamiltonian numerically by using a modified Lanczos technique (see Ref. 14 for details).

III. LUTTINGER LIQUID TO CDW TRANSITION

The spin Hamiltonian H_{eff}^{spin} in Eq. (5) with $J_2=0$, i.e., without NNN interaction, has been shown to undergo a LL to CDW state transition at zero magnetization ($\Sigma_j\sigma_j^z=0$) when $J^z=2J_1$ and at nonzero magnetization is always a LL.[15] On including a nonzero J_2, the disordering effect increases because the NNN interaction is only in the transverse direction and the LL to CDW transition will occur at higher values of J^z. We expect that including J_2 does not change the universality class and that the central charge $c=1$.

We first study the static spin-spin correlation function on rings with an even number of sites N and extract information about the critical exponent. The static spin-spin correlation function for a chain of length N is given by $W_l(N)=(4/N)\Sigma_{i=1}^{N}\langle S_i^zS_{i+l}^z\rangle$ and has the asymptotic behavior $\lim_{N\to\infty}W_l(N)\approx A(-1)^l/l^{\eta}$ for the anisotropic Heisenberg model when $l\gg 1$.[16] Furthermore, A is an unknown constant and $1<\eta\leqslant 2$ when the system is in the disordered (or LL) state, $\eta=1$ is the transition point to the antiferromagnetic (CDW) state, and $\eta=0$ means the system is totally antiferromagnetic (or CDW).

We will now derive an analytic expression for the critical exponent η based on the work of Luther and Peschel.[16] The effective polaronic Hamiltonian given by Eq. (4) can be written in momentum space as

$$\begin{aligned}H_{eff}^{pol}=&-2J_1\sum_k\cos(k)c_k^{\dagger}c_k+\frac{J^z}{N}\sum_q\cos(q)\rho(q)\rho(-q)\\&-\frac{4J_2}{N}\sum_{k,k',q}\cos(k+k')c_{k+q}^{\dagger}c_{k'}^{\dagger}c_{k'+q}c_k\\&-2J_2\sum_k\cos(2k)c_k^{\dagger}c_k,\end{aligned}\tag{6}$$

where $\rho(q)=\Sigma_pc_{q+p}^{\dagger}c_p$. Furthermore, constant terms have been ignored. Next, we linearize the kinetic energy term close to the Fermi points and follow it up with the bosonization procedure. Then on taking exchange effects into account, as pointed out by Fowler,[17] we obtain the following bosonized Hamiltonian:

$$\begin{aligned}H_{bos}^{pol}=&\left[\frac{4\pi J_1+4J^z+8J_2}{N}\right]\sum_{k>0;i=1,2}\rho_i(k)\rho_i(-k)\\&+\left[\frac{8J^z-32J_2}{N}\right]\sum_{k>0}\rho_1(k)\rho_2(-k).\end{aligned}\tag{7}$$

It is important to note that only the forward scattering part involving the coefficient J^z contributes to the self-energy correction.

Now, to calculate the critical exponent η, we will follow the usual procedure and diagonalize the bosonized Hamiltonian of Eq. (7) using the following transformations:

$$\rho_1(k)=\bar{\rho}_1(k)\cosh\phi+\bar{\rho}_2(k)\sinh\phi$$

and

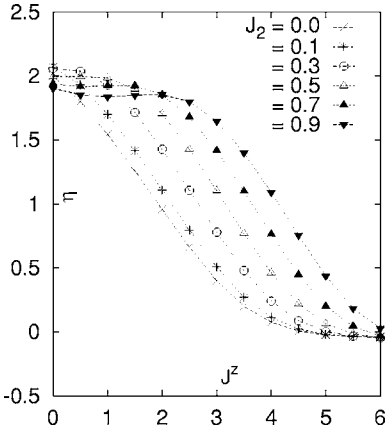

FIG. 1. Plot of spin-spin correlation exponent for various values of J^z and J_2. The dashed lines are guides to the eye.

$$\rho_2(k) = \bar{\rho}_2(k)\cosh\phi + \bar{\rho}_1(k)\sinh\phi.$$

Then, on setting the coefficient of the off-diagonal term equal to zero in the transformed Hamiltonian, we get

$$\tanh 2\phi = -\frac{2J^z - 8J_2}{2\pi J_1 + 2J^z + 4J_2}. \tag{8}$$

Using Eq. (8) we obtain

$$\eta = 2e^{2\phi} = 2\left[\frac{1 + 6J_2/\pi J_1}{1 + 2J^z/\pi J_1 - 2J_2/\pi J_1}\right]^{1/2}. \tag{9}$$

IV. RESULTS AND DISCUSSION

It is known that for an anisotropic Heisenberg spin chain, when $N/2$ is even the correlation function goes to zero smoothly as the longitudinal interaction goes to zero.[18] Hence we have calculated $W_{N/2}(N)$ only for odd values of $N/2$ with $N=6$, 10, 14, 18, and 22 at $J_1=1$ and different values of J^z and J_2. Using a linear least squares fit for a plot of $\ln W_{N/2}(N)$ versus $\ln N$ we obtained the value of η from the slope at each value of J^z and J_2. The error in η for all curves is within ≈ 0.05 and hence verifies that one has the expected quasi-long-range order. For $J^z=2$ and $J_2=0$ we get $\eta=0.96\pm0.05$ which includes the exact value of $\eta=1$ obtained from the Bethe ansatz. Thus we expect the η values obtained by our procedure to be reasonably accurate. Since for $J^z>2$ and $J_2=0$ we obtain a CDW state, by increasing J_2 at any $J^z>2$ we should increase the disordering effect and hence we see in Fig. 1 that the η value increases. We find that for $J^z\approx 6$ the value of η becomes slightly negative but with magnitude within the error of 0.05. At higher J^z values (≈ 10 and higher) η tends to zero. At small values of J^z ($\leqslant 0.5$) as J_2 increases initially η increases even to values above 2 and then decreases to values below 2. We think that this interesting feature occurs because smaller values of J_2 enhance disorder while larger values of J_2 increase correlations. However, the behavior at $J^z=0$ and $J_2>0$ needs further understanding. Our derived analytic expression, reliable at small values of J_2/J_1 and $\eta<2$, shows that η does increase with increasing values of J_2 and gives values reasonably close to the numerical ones for $J^z/J_1<1$.

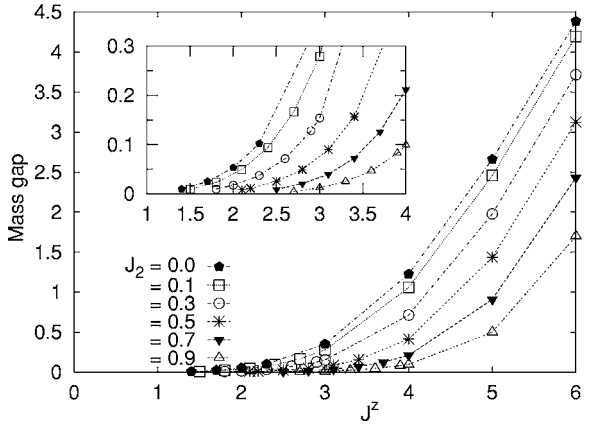

FIG. 2. Mass gap dependence on J^z and J_2.

We will now consider the mass gap, at the half-filled state for the Hamiltonian $H=H_{eff}^{pol}+g^2\omega_0\Sigma_j n_j$ [see Eq. (4)], defined as twice the energy difference between the ground state with $1+N/2$ electrons and the ground state of the $N/2$ electronic system. The mass gap is calculated for rings with $N=10$, 12, 14, 16, 18, and 20 sites. Including $N=6$ and 8 only increases the error. The mass gap plot in Fig. 2 is obtained using finite-size scaling by plotting the mass gap versus $1/N$ and extrapolating the linear least squares fit to the value corresponding to $1/N=0$. In the plot the size of the symbol is larger than the error. From the inset of the plot of mass gap versus J^z at various values of J_2, we see that the mass gap goes to zero at $J^z\approx 1.4$ at $J_2=0$ which is a significant underestimation of the transition value of $J^z=2$. Also on comparing with Fig. 1, we again notice that the LL to CDW transition value of J^z at different J_2 values is grossly underestimated. Furthermore, as expected, the mass gap increases (decreases) monotonically with J^z (J_2) at a fixed J_2 (J^z).

We will now discuss the region of validity for our model, given by Eq. (4) and as depicted in Fig. 3 (region above the lower curve), in the two-dimensional parameter space of g and t/ω_0. First, since we use the assumption that $\omega_0 \gg J_1$ in our derivation, we choose the validity condition as $\omega_0 \geqslant 10J_1$. Next, we would like the second-order energy term

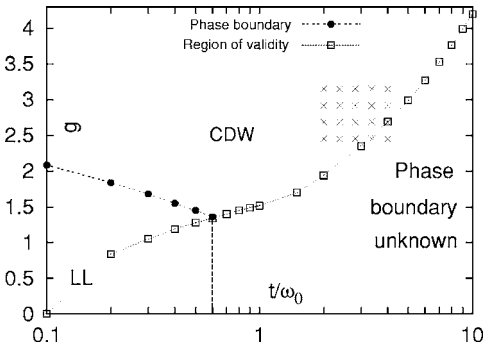

FIG. 3. Plot of region of validity boundary and LL-CDW phase boundary for g versus t/ω_0. The errors are smaller than the symbols. The crosses depict realistic regime.

$E^{(2)}$ in the perturbation series to be much smaller than the unperturbed term $E_{0,0}$. We find that for $t/\omega_0 \leqslant 1$, the condition $\omega_0 = 10J_1$ produces a boundary on which the ratio $E_{0,0}/E^{(2)} > 5$ with the ratio increasing rapidly as t/ω_0 decreases. As for $t/\omega_0 \geqslant 2$, we find that the condition $g^2\omega_0 \geqslant 3J^z$ is more restrictive than the first one ($\omega_0 \geqslant 10J_1$) and produces a ratio of $E_{0,0}/E^{(2)} > 3$ at the boundary. Next we will discuss the LL to CDW phase transition boundary obtained from $\eta = 1$ condition and depicted by the upper curve in Fig. 3. We find that the phase transition points lie within the region of validity only for $t/\omega_0 \leqslant 0.6$. In the region to the right of the dashed vertical line and below the region-of-validity curve the phase boundary cannot be determined using our model. It is important to note that the experimentally realistic parameter regime $6 < g^2 < 10$ and $2 < t/\omega_0 < 4$ lies mostly inside the region of validity. Upon comparing our numerical phase transition results with those of Bursill *et al.*,[19] we find that for small values of $t/\omega_0 \leqslant 0.1$ the critical g_c values agree well. However for larger values the results do not agree. At $t/\omega_0 = 0.5$ our $g_c = 1.45 \pm 0.02$ (with $E_{0,0}/E^{(2)} > 17$ and $\omega/J_1 > 15$) is noticeably smaller than the $g_c = 1.63(1)$ of Ref. 19 and at $t/\omega_0 = 1$ we find that $g_c < 1.52$ whereas Bursill *et al.* get $g_c = 1.61(1)$. As for $t/\omega_0 \geqslant 2$, our region of validity lies above the phase transition boundary given in Ref. 19. However, interestingly, the numerical estimates of the critical g_c by Hirsch and Fradkin[12] are consistent with our results, with their g_c value agreeing with ours at $t/\omega_0 = 0.5$, while at higher values of t/ω_0 their g_c values lie outside our region of validity.

Now that the region of validity has been identified, we will analyze within this region the small parameter for our pertubation theory. For $g > 1$, one approximates $f_1(g) \sim e^{g^2}/g^2$ and $[2f_1(g) + f_2(g)] \sim e^{2g^2}/2g^2$ with the approximations becoming exact in the limit $g \to \infty$. Then the effective polaronic Hamiltonian of Eq. (4), for the case $g > 1$, simplifies to

$$H_{eff}^{pol} \sim -g^2\omega_0 \Bigg(\sum_j n_j + \zeta e^{-g^2} \sum_j (c_j^\dagger c_{j+1} + \text{H.c.}) + \zeta^2 e^{-g^2} \sum_j \{c_{j-1}^\dagger (1 - 2n_j) c_{j+1} + \text{H.c.}\} + \zeta^2 \sum_j n_j (1 - n_{j+1}) \Bigg), \tag{10}$$

where $\zeta \equiv t/g^2\omega_0$ is the polaron size parameter. In the region of validity for our model, when the adiabaticity parameter $t/\omega_0 > 0.2$, we have the constraints $g > 1$ and $g^2\omega_0 \geqslant 2t$. Thus we see that, for the region $t/\omega_0 > 0.2$, the polaron size parameter ζ is the small parameter.

Now, for the extreme antiadiabatic regime of $t/\omega_0 \leqslant 0.1$, all values of g are allowed by our model. When $g > 1$, again Eq. (10) is valid with the same small parameter ζ. However, when $g < 1$, we make the approximations $f_1(g) \sim g^2$ and $[2f_1(g) + f_2(g)] \sim 2f_1(g)$ with the approximations becoming exact in the limit $g \to 0$. Then, for $g < 1$, the effective polaronic Hamiltonian given by Eq. (4) becomes

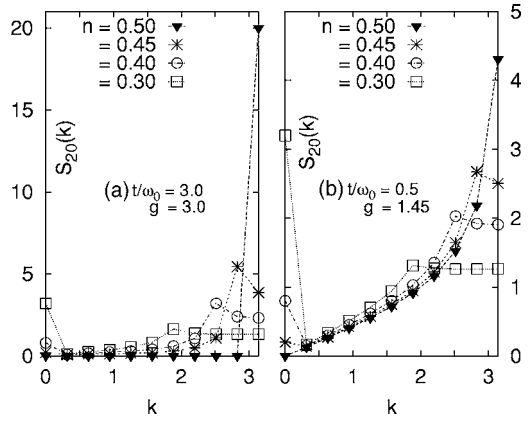

FIG. 4. Structure factor plots at various values of k and n.

$$H_{eff}^{pol} \sim -g^2\omega_0 \Bigg[\sum_j n_j + \zeta e^{-g^2} \sum_j (c_j^\dagger c_{j+1} + \text{H.c.}) + \left(\frac{t}{\omega_0}\right)^2 e^{-2g^2} \sum_j \{c_{j-1}^\dagger (1 - 2n_j) c_{j+1} + \text{H.c.}\} + 4\left(\frac{t}{\omega_0}\right)^2 e^{-2g^2} \sum_j n_j (1 - n_{j+1}) \Bigg]. \tag{11}$$

Thus, for the regime $t/\omega_0 \leqslant 0.1$ and $g < 1$, the adiabaticity parameter t/ω_0 is the small parameter in Eq. (11) with $g \sim 1$ corresponding to small polarons and $g \to 0$ (such that $g^2\omega_0 \ll t$) corresponding to large polarons.

Finally, we also study the static structure factor $S_N(k) \equiv \Sigma_{l=1}^N e^{ikl} W_l(N)$. The structure factor offers information about the correlation lengths even in the LL phase at all filling factors n. In fact, the correlation length decreases with increasing width of the structure factor near its peak at $2\pi n$. We first observe that $\Sigma_k S_N(k) = N$ and that $S_N(0) = 4N(n - 0.5)^2$, both of which are borne out by both the plots in Fig. 4 done at $N = 20$. The plots are only for $k = 2\pi m/N$ with $m = 0, 1, \ldots, N/2$ as $S_N(k)$ is symmetric about π, and are only for $n \leqslant 0.5$ because of particle-hole symmetry. Figure 4(b), plotted for $t/\omega_0 = 0.5$ and $g = g_c = 1.45$ (or $J^z = 2.53$ and $J_2 = 0.245$), corresponds to the LL-CDW transition point at $n = 0.5$, while Fig. 4(a), done for the realistic values of $t/\omega_0 = 3$ and $g = 3$ (or $J^z \approx 3000$ and $J_2 \approx 0.38$), depicts the situation deep inside the CDW phase at $n = 0.5$. Now, we know that at $n = 0.5$, the structure factor $S_N(\pi) \sim \int dl/l^\eta$ and hence diverges for $\eta \leqslant 1$ (CDW regime) as $N \to \infty$ with the divergence being faster as we go deeper inside the CDW regime. Also the structure factor remains finite at $2\pi n$ for all other filling factors even when $N \to \infty$ because here the system is always a LL. From plot (a) we infer that deep inside the CDW state $S_N(\pi) \approx N$ and $S_N(k \neq \pi) \approx 0$. As for the CDW transition point depicted in plot (b) at $n = 0.5$, the structure factor peaks sharply but more gradually at $k = \pi$. In both plots the largest peak occurs for $n = 0.5$ with peak size diminishing and curve width increasing as values of n decrease. Thus, we see that for $n \neq 0.5$ also, short-range correlations exist with the correlation length decreasing as the deviation from half filling increases.

Lastly and importantly, using arguments similar to those in the 1D case, we have also derived the effective polaronic Hamiltonian in d dimensions to be[20]

$$H_{eff}^{pol} = -g^2\omega_0 \sum_j n_j - J_1 \sum_{j,\delta} c_j^\dagger c_{j+\delta} - J_2 \sum_{j,\delta,\delta' \neq \delta} c_{j+\delta'}^\dagger (1-2n_j) c_{j+\delta} - 0.5 J^z \sum_{j,\delta} n_j (1-n_{j+\delta}), \tag{12}$$

where δ corresponds to the nearest neighbor.[21]

In conclusion, we have derived an effective polaronic Hamiltonian for the spinless 1D Holstein model which is found to be valid in most of the experimentally realistic regime. We mapped the effective Hamiltonian onto a next-to-nearest-neighbor anisotropic Heisenberg Hamiltonian. Using the modified Lanczos technique extensively, we computed the static spin-spin correlation exponent η and the mass gap at half filling for general values of the parameters in the effective spin Hamiltonian. The mass gap values were found to significantly underestimate the critical electron-phonon coupling g_c. In contrast, the η values were found to give reliable estimates of g_c and consequently were used to determine the LL-CDW quantum phase transition. The structure factor calculations revealed that the correlation length diminishes with increasing deviation from half filling. Lastly, our approach, exact to second order in perturbation, is extended to obtain an effective polaronic Hamiltonian in d dimensions also. Our work opens up a whole host of future challenges such as (1) extension to finite temperatures and studying the metal-insulator transition; (2) including the Hubbard interaction U; (3) analyzing the d-dimensional model in Eq. (12);[20] and (4) deriving an analogous effective Hamiltonian for Jahn-Teller systems.

[1] T. Holstein, Ann. Phys. (N.Y.) **8**, 343 (1959).

[2] A. S. Alexandrov and N. Mott, *Polarons and Bipolarons* (World Scientific, Singapore, 1995).

[3] A. Alexandrov and J. Ranninger, Phys. Rev. B **23**, 1796 (1981); A. S. Alexandrov, J. Ranninger, and S. Robaszkiewicz, *ibid.* **33**, 4526 (1986).

[4] The many-polaron problem was studied for the spinless Frohlich model (within a first-order perturbation treatment) by A. S. Alexandrov and P. E. Kornilovitch, J. Phys.: Condens. Matter **14**, 5337 (2002). These authors examine the case of infinite-range electron-phonon coupling with zero on-site interaction, whereas we deal with the complementary on-site-interaction-only case.

[5] For a review see *Colossal Magnetoresistance, Charge Ordering, and Related Properties of Manganese Oxides*, edited by C. N. R. Rao and B. Raveau (World Scientific, Singapore, 1998).

[6] These results will be reported elsewhere by the authors (unpublished).

[7] T. Ishiguro, K. Yamaji, and G. Saito, *Organic Superconductors* (Springer, Berlin, 1998); N. Tsuda, K. Nasu, A. Yanase, and K. Siratori, *Electronic Conduction in Oxides* (Springer, Berlin 1990).

[8] I. G. Lang and Yu. A. Firsov, Zh. Eksp. Teor. Fiz. **43**, 1843 (1962) [Sov. Phys. JETP **16**, 1301 (1962)].

[9] S. Yarlagadda, Phys. Rev. B **62**, 14828 (2000).

[10] F. Marsiglio, Physica C **244**, 21 (1995).

[11] W. Stephan, Phys. Rev. B **54**, 8981 (1996).

[12] J. E. Hirsch and E. Fradkin, Phys. Rev. B **27**, 4302 (1983).

[13] For a review see I. Bose, in *Field Theories in Condensed Matter Physics*, edited by Sumathi Rao (Institute of Physics Publishing, Bristol, 2002).

[14] E. R. Gagliano, E. Dagotto, A. Moreo, and F. C. Alcaraz, Phys. Rev. B **34**, 1677 (1986); *ibid.* **35**, 5297 (1987).

[15] F. D. M. Haldane, Phys. Rev. Lett. **45**, 1358 (1980).

[16] A. Luther and I. Peschel, Phys. Rev. B **12**, 3908 (1975).

[17] M. Fowler, J. Phys. C **13**, 1459 (1980).

[18] E. Lieb, T. Schultz, and D. Mattis, Ann. Phys. (N.Y.) **16**, 407 (1961).

[19] R. J. Bursill, R. H. McKenzie, and C. J. Hamer, Phys. Rev. Lett. **80**, 5607 (1998).

[20] The infinite-dimensional case will be analyzed elsewhere by the authors (unpublished).

[21] For a study of the energy dispersion of a single small polaron in two dimensions by resummed strong-coupling perturbation theory see Ref. 11 and by exact quantum Monte Carlo calculations see P. E. Kornilovitch and A. S. Alexandrov, Phys. Rev. B **70**, 224511 (2004).